

# Refractive index properties of SiN thin films and fabrication of SiN optical waveguide

D. S. Kim · S. G. Yoon · G. E. Jang · S. J. Suh · H. Kim · D. H. Yoon

Received: 27 June 2005 / Revised: 13 June 2006 / Accepted: 7 July 2006  
© Springer Science + Business Media, LLC 2006

**Abstract** SiN thin films having excellent surface morphology for the optical device application were synthesized using a plasma enhanced chemical vapor deposition (PECVD) method at low temperature (350°C) using silane (SiH<sub>4</sub>) and nitrogen (N<sub>2</sub>). The effects of the SiH<sub>4</sub>/N<sub>2</sub> flow ratio, rf power and annealing on the SiN films were investigated. The optical and structural properties of SiN films were characterized using an ellipsometry, a fourier-transform infrared spectroscopy (FT-IR), and an atomic force microscope (AFM). The refractive index increased from 1.6 to 2.3 as the SiH<sub>4</sub>/N<sub>2</sub> ratio was increased from 0.17 to 1.67. The rms surface roughness decreased from 14.1 to 3.6 Å after post-deposition annealing process performed at 800°C for 1 hr in an air ambient. We could fabricate straight waveguides based on a three layer structure and have no problems with step coverage.

**Keywords** Silicon nitride (SiN) · PECVD · Refractive index · Optical waveguide

## 1 Introduction

Recently, SiO<sub>2</sub> and SiO<sub>x</sub>N<sub>y</sub> films are being widely used as optical waveguide materials for various optical devices, such as optical splitters and de-multiplexers [1–4]. However, the miniaturization of the device size, very large-scale integration, and high optical efficiency are continuously required for

the future generation of optical devices. Among many possible material systems, silicon nitride (SiN) is one of good candidates especially for thin film optical devices due to its good chemical stability, high refractive index, and low optical loss [5]. Silicon waveguides are compatible with all of the above requirements, with the exception of dimensional integrity. The ideal cladding material is SiO<sub>2</sub>, however the required submicron feature sizes of silicon waveguides and passive devices cannot yet be reliably created with low surface roughness. In order to validate the design principles and prototype the microphotonic circuit functionality, SiN waveguides represent a suitable compromise between index contrast and dimension control.

In particular, the utilization of SiN films deposited by plasma enhanced chemical vapor deposition (PECVD) at low temperatures for the fabrication of optical devices has become very attractive, due to the possibility of integrating the optical and electrical devices in the same chip [6–8]. Moreover, PECVD provides such advantages as high throughput, good uniformity, and excellent reproducibility. Moreover, the fundamental advantage of this technique is that it enables the control of structural, mechanical and optical properties of the deposited films by adjusting the deposition parameters [9–11].

In this paper, we studied the effect of the SiH<sub>4</sub>/N<sub>2</sub> flow ratio, rf power and post-annealing on the refractive index, the deposition rate and the surface morphology of SiN films grown by PECVD for the application of low loss optical waveguides.

## 2 Experiment

The SiN films were deposited by PECVD using a gaseous mixture of silane (10% SiH<sub>4</sub>) and nitrogen (99.999% N<sub>2</sub>).

D. S. Kim · S. G. Yoon · S. J. Suh · H. Kim · D. H. Yoon (✉)  
Department of Advanced Materials Engineering, Sungkyunkwan  
University Suwon 440-746, Korea  
e-mail: dhyoon@skku.edu

G. E. Jang  
Department of Materials Science & Materials Engineering,  
Chungbuk University Cheongju 361-763, Korea

The PECVD system has a parallel planar discharge system, which uses a rectangular rf electrode (lower) and a substrate electrode (upper). The substrate is placed on the tray with the surface to be coated facing downward, so that the deposition of dust particles and flakes can be minimized during the PECVD process.

P-type Si wafers with (100) orientations were used as substrates. Before the SiN deposition, a pre-cleaning of the wafer was performed *in-situ* in order to improve the adhesion of the film on the substrate using N<sub>2</sub> discharge with an rf power of 60 W. The chamber pressure of 0.75 torr and the temperature of 350°C were maintained during the deposition. After the deposition of the SiN layer, the films were annealed at 800°C in an air ambient for 1 hr. The effects of the SiH<sub>4</sub>/N<sub>2</sub> flow ratio, rf power and annealing conditions on the properties of the SiN films were investigated afterwards.

The refractive index and the thickness of the SiN films were measured using an ellipsometer operating at a wavelength of 1550nm. Fourier-transform infrared spectroscopy (FT-IR) was used to determine the composition of the SiN films and atomic force microscopy (AFM) was used to analyze the surface morphology.

### 3 Results and discussion

Figure 1 shows the variation of the refractive index and the deposition rate of SiN films as a function of SiH<sub>4</sub>/N<sub>2</sub> flow ratio. The change of the refractive index of SiN film with and without a post-annealing is also included. The refractive index of SiN film continuously increased with the increase of SiH<sub>4</sub>/N<sub>2</sub> flow ratio at an rf power level of 30W. However, the deposition rate showed a continuous decrease after a slight increase before the certain critical point around a mixing ratio of 0.6. The increase of the refractive index can be explained by the formation of Si-rich radicals with the

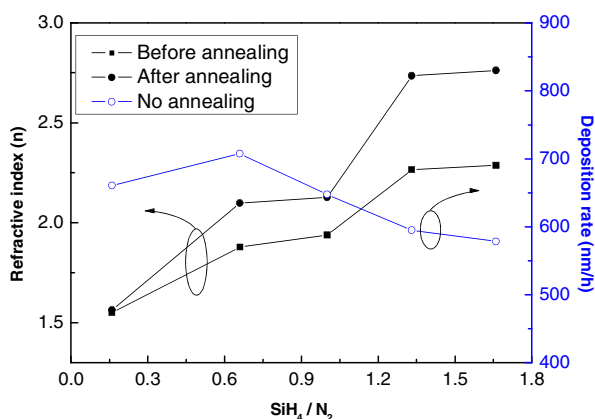


**Fig. 1** Variation of refractive indices and deposition rate as a function of SiH<sub>4</sub>/N<sub>2</sub> ratio

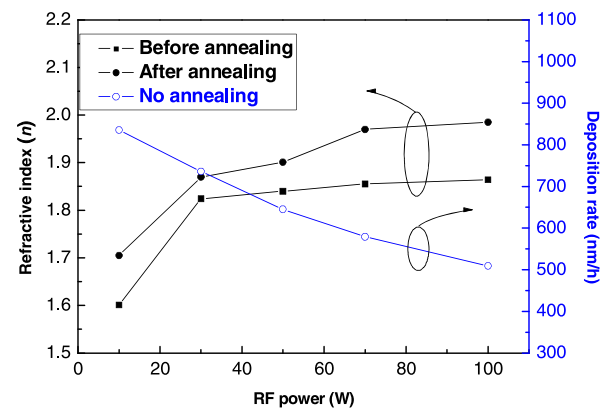


**Fig. 2** Variation of refractive indices and deposition as a function of rf power

increase of SiH<sub>4</sub>/N<sub>2</sub> flow ratio [12]. For the deposition rate of the SiN films, the initial slight increase can be explained by the disintegration of rich radicals due to the plasma effect [13]. Rich radicals supply materials needed for the formation of the SiN film and allow the deposition process to continue. However, the deposition rate decreased when the number of these rich radicals was increased. The subsequent decrease in the deposition rate is believed to be due to the disturbance of a limited number of very rich radicals on the surface when the deposition rate reached a critical value. These very rich radicals may disturb the SiN deposition process when the SiH<sub>4</sub>/N<sub>2</sub> flow ratio was increased. As a result, the deposition rate increased up to 708nm/hr and then subsequently decreased when the SiH<sub>4</sub>/N<sub>2</sub> flow ratio reached a value of 1.

Figure 2 shows the deposition rate and the refractive index for the SiN films as a function of the rf power were measured after fixing the SiH<sub>4</sub>/N<sub>2</sub> flow ratio at 1. With the increase of the rf power, the deposition rate continuously decreased due to the occurrence of a strong radical stream on the film

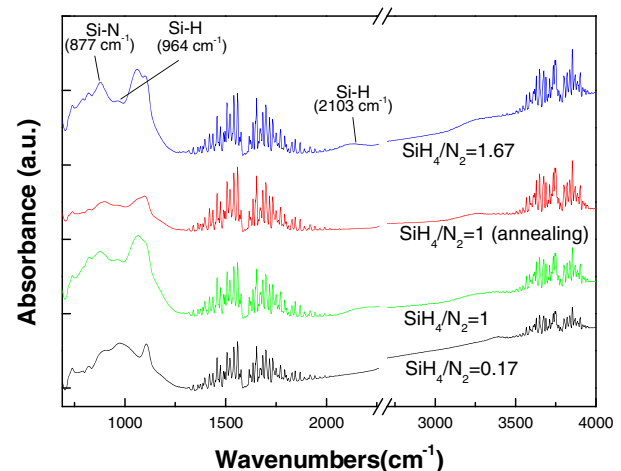


**Fig. 3** FT-IR spectra as a function of SiH<sub>4</sub>/N<sub>2</sub> flow ratio and post-annealing

surface, however, the refractive index increased due to the huge generation of Si radicals. It suggests that Si-rich  $\text{Si}_3\text{N}_4$  films may form until perfect nitride of the Si radicals occurs with the increase of rf power. The refractive index increased from 1.60 to 1.86 due to more efficient nitride of the Si radicals when the rf power was increased from 10 to 100W.

The effects of different  $\text{SiH}_4/\text{N}_2$  flow ratio and the post-annealing on FT-IR absorbance spectra of SiN films is displayed in Fig. 3. When the  $\text{SiH}_4/\text{N}_2$  flow ratio was increased from 0.17 to 1, the intensities of Si-N ( $877\text{cm}^{-1}$ ) and Si-H ( $964\text{cm}^{-1}$ ,  $2103\text{cm}^{-1}$ ) peaks increased indicating the generation of Si-rich radicals, which in turn indicates the increase of deposition rate as observed in Fig. 1. However, when the  $\text{SiH}_4/\text{N}_2$  flow ratio was increased from 1 to 1.67, the magnitude of increment of Si-N and Si-H peak intensities was less than that observed at lower  $\text{SiH}_4/\text{N}_2$  flow ratios. This reflects the disturbance of the film deposition process by the excessive generation of Si radicals at higher  $\text{SiH}_4/\text{N}_2$  flow ratios, which results in the decrease of the deposition rate. After post-annealing, the Si-H peaks of the FT-IR absorbance spectra disappeared. Therefore, the increase of the refractive index after the annealing of the SiN thin films may be attributed to a decrease of hydrogen content and an increase of the film density [14].

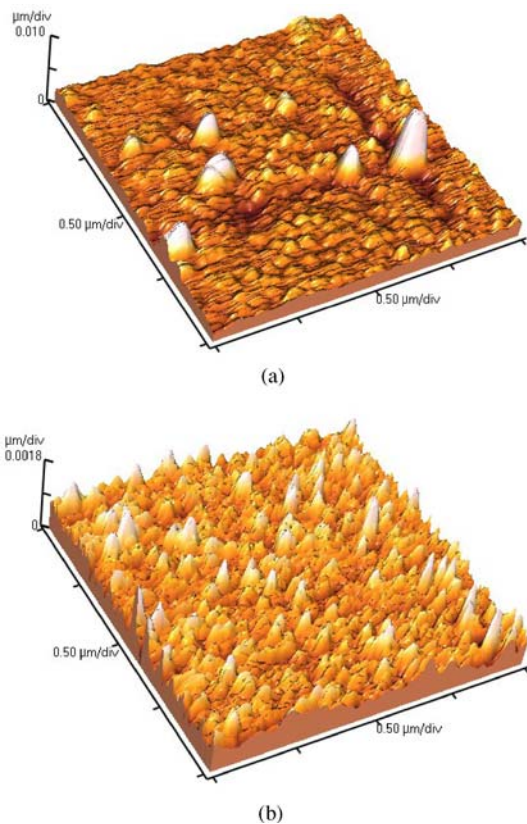


**Fig. 4** AFM images ( $2 \times 2\mu\text{m}$ ) of SiN films (a) before annealing (rms roughness:  $14.11\text{\AA}$ ) and (b) after annealing (rms roughness:  $3.577\text{\AA}$ )



**Fig. 5** The SiN optical waveguide (a) cross-sectional SEM images and (b) the input near-field output pattern shown on the display monitor of an infrared camera (mode image of straight waveguide)

Figure 4 shows the AFM images of the SiN thin films before and after annealing when the  $\text{SiH}_4/\text{N}_2$  flow ratio and the rf power were fixed at 1 and 30W, respectively. Comparing the surface morphology before and after annealing, the rms (root-mean-square) roughness of SiN films decreased from  $14.1$  to  $3.6\text{\AA}$  after annealing. Therefore, the surface morphology of the SiN thin films could be significantly improved by post-annealing process. Lowering of the rms roughness and the reduction of the number of hydrogen bonds by the thermal annealing process are expected to be an efficient way to improve the scattering and absorption loss characteristics of SiN film [15].

Figure 5 shows the SiN optical waveguide (a) cross-sectional SEM images and (b) the input near-field output pattern. Preliminary optical measurements were carried out on the some sample. A  $1552\text{ nm}$  HeNe laser was fired into the cleaved end of the waveguide via a microscope objective lens. The emerging light was picked up on an IR camera and displayed on screen. Figure 5(b) shows the light emerging from the end of the waveguide. If the fiber spot size is well matched to that of the fiber, and also optimally aligned with the waveguide, there is minimal mismatch between the fundamental modes of the fiber and waveguide, with transmission losses

typically around 0.1 dB of loss. However, if the fiber and the waveguide spot sizes are offset or tilted, the transmission loss will be considerably high. This result illustrates that the mode of output is a waveguiding single-mode.

#### 4 Conclusion

SiN thin films having optically low loss were grown by PECVD process with various conditions of SiH<sub>4</sub>/N<sub>2</sub> flow ratio and rf power, and the post-annealing effect was investigated. The deposition rate of SiN thin films was about 509~835nm/h in the range of SiH<sub>4</sub>/N<sub>2</sub> flow ratio and rf power investigated in this study. The reflective index of the SiN thin film was increased with the increase of SiH<sub>4</sub>/N<sub>2</sub> flow rate and rf power. The increase of rf power increased the deposition rate in PECVD regime, however, in this experimental condition the increase of radical stream showed a reverse effect. We found that the surface roughness could be improved by the post-annealing process, and also the absorption loss and scattering optical loss of the SiN thin film could be minimized by the hydrogen removal mechanism through the annealing process. Straight waveguides based on a three layer structure are relatively easy to fabricate and have no problems with step coverage. The emerging light was picked up on an IR camera and displayed on a screen, showing that most of the light is confined within the waveguide. This illustrates that the output intensity mode corresponds to that of a single-mode waveguide.

**Acknowledgements** The paper was supported by Samsung Research Fund, Sungkyunkwan University, 2004.

#### References

1. J. Zhang, Z. Ren, R. Liang, Y. Sui, and W. Liu, *Surf. Coat. Technol.*, **131**, 116 (2000).
2. H. Uetsuka, K. Akiba, K. Morosawa, H. Okano, S. Takasugi, and K. Inaba, *IEICE Trans. Electron.* **E80 C**, 6194 (1997).
3. Y.T. Kim, S.M. Cho, H.Y. Lee, H.D. Yoon, and D.H. Yoon, *Surf. Coat. Technol.*, **174**, 166 (2003).
4. M. Kawachi, *Opt. Quantum Electron.*, **22**, 391 (1990).
5. H.A. Haus, L.C. Kimerling, and M. Romagnoli, *ECOC-IOOC. We1.2*, 1 (2003).
6. Kanji Yasui, Masaaki Nasu, Kazuki Komaki, and Shigeo Kaneda, *Jpn. J. Appl. Phys.*, **29**, 918 (1990).
7. A. Borghesi, A. Sassella, B. Pivac, and L. Zanotti, *Solid-State Commun.*, **100**, 657 (1996).
8. A. Sassella, A. Borghesi, F. Corni, A. Monelli, G. Ottaviani, R. Tonini, B. Pivac, M. Bacchetta, and L. Zanotti, *J. Vac. Sci. Technol., A* **15**, 377 (1997).
9. D.D. Sala and G. Fortunato, *J. Electrochem. Soc.*, **137**, 2550 (1990).
10. H.J. Schliwinski, U. Schnakenberg, W. Kindbracke, H. Neff, and P. Lange, *J. Electrochem. Soc.*, **139**, 1730 (1992).
11. K. Wörhoff, A. Driessen, P.V. Lambeck, L.T.H. Hilderink, P.W.C. Linders, and T.J.A. Popma, *Sensor Actuators A: Phys.*, **74**, 9 (1999).
12. R.S. Rosler, et al., *Solid State Technol.*, **24**(4), 172 (1981).
13. H. Dun, P. Pan, F.R. White, and R.W. Douse, *J. Electrochem. Soc.*, **128**, 1555 (1981).
14. M. Saga, et al., Plasma Processing, J. Dieleman, R. Frieser, and G.S. Mathad, Eds., Electrochemical Society, Penning. N.J., **486** (1982).
15. Y.T. Kim, S.M. Cho, Y.G. Seo, H.D. Yoon, Y.M. Im, and D.H. Yoon, *Surf. Coat. Technol.*, **173**, 204 (2003).